Steel and Composite Structures, *Vol. 24, No. 6 (2017) 697-709*
DOI: https://doi.org/10.12989/scs.2017.24.6.697

Shear buckling analysis of laminated plates on tensionless elastic foundations

Jianghui Dong [a], Xing Ma [*], Yan Zhuge [b] and Julie E. Mills [c]

School of Natural and Built Environments, University of South Australia, Adelaide, SA 5095, Australia

(*Received January 24, 2017, Revised April 27, 2017, Accepted May 18, 2017*)

Abstract. The current study addresses the local buckling analysis of an infinite thin rectangular symmetrically laminated composite plate restrained by a tensionless Winkler foundation and subjected to uniform in-plane shear loading. An analytic method (i.e., one-dimensional mathematical method) is used to achieve the analytical solution estimate of the contact buckling coefficient. In addition, to study the effect of ply angle and foundation stiffness on the critical buckling coefficients for the laminated composite plates, the parametric studies are implemented. Moreover, the convergence for finite element (FE) mesh is analysed, and then the examples in the parametric study are validated by the FE analysis. The results show that the FE analysis has a good agreement with the analytical solutions. Finally, an example with the analytical solution and FE analysis is presented to demonstrate the availability and feasibility of the presented analytical method.

Keywords: buckling coefficient; contact buckling; finite element analysis; Winkler foundation; laminated composite plate

1. Introduction

It is well known that laminated composite structures have been widely applied in a variety of engineering fields, such as aerospace, marine, automotive and building structures, because of the specific advantages of being lightweight with high stiffness. Of these, rectangular laminated composite plates and panels are becoming increasingly used in industrial fields as load carrying elements. It is essential to analyze and consider the local buckling problem of rectangular laminated composite plates and panels to ensure reliably designed and safe applications.

Based on Timoshenko and Gere's thin plate theory (Timoshenko and Gere 1936), the buckling problems of laminated composite plates have been studied by a number of researchers. Kosteletos (1992) studied the initial buckling of a finite long thin laminated composite plate subjected to compressive and in-plane shear loading. Nemeth investigated the buckling of a long symmetrically laminated composite plate subjected to compressive and in-plane shear loading (Nemeth 1992) and linearly varying axial edge and in-plane shear loading (Nemeth 1997). Weaver (2004) analyzed the local buckling of a long rectangular plate under in-plane shear. Darvizeh *et al*. (2002) used the differential quadrature method to analyse the buckling of composite plates. Ashour (2003) investigated the effect of edges elastically restrained on buckling of laminated composite plate. Qiao and Huo (2011) illustrated the buckling analysis of an infinite thin rectangular orthotropic restrained plate for different edges conditions under uniform shear forces. Altunsaray and Bayer (2014) studied the buckling problem of symmetrically laminated plate using Galerkin and finite difference method. The nth-order shear deformation theory (Bechri *et al*. 2016) and higher order shear deformation plate theory (Baseri *et al*. 2016) were considered to study the buckling of laminated plates.

In industrial practise, the laminated plate can be employed as skin elements when combined with relative soft core materials to form new structural composite components. When subjected to compression and/or shear loads, the skin element might buckle together with the core materials if there is sufficient bonding strength between the skin and the core material. This phenomenon is a kind of bilateral buckling, where a general eigenvalue solution can be achieved through finite element analysis. However, if delamination occurs between the skin and the core materials, parts of the skin might buckle away, while other parts still remain contact with the core material. This phenomenon is named unilateral contact buckling, also known as delamination buckling. The analysis is more complicated due to the unknown boundary conditions in the system, i.e., the unknown contact or noncontact zones.

For contact buckling problems, quite a few researches have been done on flat isotropic plate and profiles plate elements. It is accepted that Seide (1958) was the first person to study the contact buckling problem of a thin plate on tensionless elastic foundations. Since then, researchers have extensively investigated the contact buckling phenomenon of plates on elastic and/or rigid foundations. The local buckling of plates constrained by rigid foundations was analysed (Uy and Bradford 1996, Wright 1993). Smith *et al*. conducted several studies, e.g., rectangular plates on rigid foundation under combined

*Corresponding author, Ph.D., Senior Lecturer,
E-mail: Xing.Ma@unisa.edu.au
[a] Ph.D., E-mail: jianghui.dong@mymail.unisa.edu.au
[b] Professor, E-mail: yan.zhuge@unisa.edu.au
[c] Professor, E-mail: julie.mills@unisa.edu.au

ISSN: 1229-9367 (Print), 1598-6233 (Online)

loadings (Smith *et al*. 1999b, c, Bradford *et al*. 2000) and flat rectangular plates on rigid foundations under only in-plane shear (Smith *et al*. 1999a, d). In a further study, a spectral method was applied to study the unilateral buckling problem of plates in elastic foundations (Muradova and Stavroulakis 2012). Arabzade *et al*. (2011) analysed the buckling of shear walls with bolts. Ma *et al*. carried out some researches on the contact buckling behaviour for rectangular plates in composite structures, e.g., local compressive buckling of thin flat plates (Ma *et al*. 2008a, b, 2007, Li *et al*. 2016, Keage *et al*. 2011); local shear buckling of thin infinite flat rectangular plates (Ma *et al*. 2011); thin infinite profiled rectangular plates (Ma *et al*. 2008c, Dong *et al*. 2016a, b).

However, regarding the contact buckling analysis of laminated plates, the research in current literature is relatively rare. The compressive buckling behaviour of laminated composite plates resting on one-sided foundations was analyse using finite elements and hierarchical Rayleigh–Ritz methods (Vaseghi *et al*. 2013). The compressive buckling of laminated composite curved panels on a Winkler foundation was studied using Rayleigh–Ritz method (Panahandeh-Shahraki *et al*. 2013). Compared with compression loading, less attention has been drawn to the contact buckling study of laminated plates subjected to in-plane shear loads. To the authors' knowledge, there has not been an analytical solution to this topic to date. The objective of the current study is to analyze the contact effect of foundation and ply angle on the local buckling of an infinite long laminated composite plate under uniform in-plane shear forces. In the current study, the contact delamination buckling of long laminated composite structures under in-plane shear loading is presented. Based on classical lamination plate theory, a one-dimensional mathematical analytic method was used to investigate the analytical solution of the local buckling of a long thin laminated composite plate constrained by Winkler foundations and imposed by pure uniform in-plane shear loading. In addition, FE analysis (using ABAQUS) was performed to validate the analytical solution. The current method and FE method were then applied to an example to further validate their effectiveness of the current method. The one-dimensional mathematical method has been used in the analysis of isotropic plate (Ma *et al*. 2011) and profiled plate (Dong *et al*. 2016a) resting on elastic tensionless foundation under in-plane shear load. However, because of the significantly different governing equation form in the case of laminated plates, solutions from literature Dong *et al*. (2016a) or Ma *et al*. (2011) are not applicable to composite plates. Meanwhile, it can be seen from the presenting here theoretical and numerical procedures, that the isotropic plate and profiled plate may be considered as special cases of laminated composite plates, meaning that solutions in this paper have more general applications than those from previous literature (Dong *et al*. 2016a and Ma *et al*. 2011).

This study is organized as following: In Section 2, the governing mathematical formulation is given, based on the classical lamination plate theory. In Section 3, numerical examples and parametric study are investigated. In Section 4, an application example of orthotropic clamped plate resting on a tensionless elastic foundation is analyzed. In Section 5, some concluding remarks are presented.

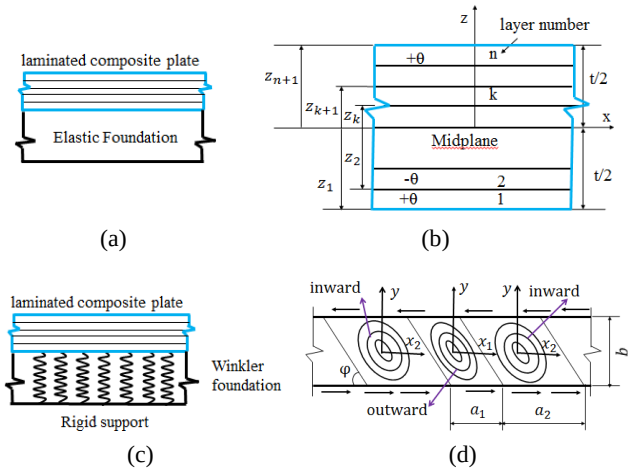

Fig. 1 Geometry of local shear buckling model: (a) symmetrical laminated composite plate on elastic foundation; (b) schematic diagram of symmetrical laminated composite plate, θ is fiber orientation angle to axis x and t is the whole plate thickness; (c) simplified model with the springs; (d) shear buckling mode of a long laminated composite plate

2. Mathematical formulation

In the current study, the local buckling problem of an infinite long symmetrically laminated composite plate restrained on a tensionless elastic foundation under uniform in-plane shear loading is studied (Fig. 1). The foundation is simplified as the springs (elastic tensionless foundation) (Fig. 1(c)). As shown in Fig. 1(d), between laminated composite plates and tensionless elastic foundations, two local coordinate systems (x_1, y, w_1) and (x_2, y, w_2) are used to demonstrate the unknown non-contact and contact zones, respectively.

Based on the classical lamination plate theory and Fig. 1, for a symmetrically laminated composite plate on foundation subjected to in-plane shear loading can be written as Eq. (1) (Ma *et al*. 2008b, Khalili *et al*. 2013, Leissa 1983, Reddy 2004, Paliwal and Ghosh 2000)

$$\begin{aligned} &D_{11}w_{i,x_ix_ix_ix_i} + 2(D_{12} + 2D_{66})w_{i,x_ix_iyy} \\ &+D_{22}w_{i,yyyy} + 4D_{16}w_{i,x_ix_ix_iy} \\ &+4D_{26}w_{i,x_iyyy} + 2N_{xy}w_{i,x_iy} = q_i \\ &|x_i| \le a_i/2 \end{aligned} \tag{1}$$

where w_i is the plate deflection (i = 1 and 2); D_{11}, D_{12}, D_{22}, D_{16}, D_{26} and D_{66} are the plate flexural stiffnesses, the definition of D_{ij}, (i, j = 1, 2, 6) is given in Appendix A (Jones 1998, Reddy 2004). The shear force N_{xy} is

$$N_{xy} = \tau_{xy}\, t \tag{2}$$

where τ_{xy} is the shear stress and t is the plate thickness.

$$q_i = \begin{cases} 0 & |x_1| \le a_1/2 \quad \text{for non-contact zone} \\ q_2(x_2, y) & |x_2| \le a_2/2 \quad \text{for contact zone} \end{cases} \tag{3}$$

Specially, if D_{16} and D_{26} can be neglected, i.e., $D_{16} = D_{26} = 0$ and $D_{11} = D_x = \frac{E^s I_{11}}{b}, D_{22} = D_y = \frac{E^s b t^3}{12 s}, 2(D_{12} + 2D_{66}) = D_{xy} = \frac{E^s t^3 s}{6(1+v^s)b}$, Eq. (1) can be simplified as the governing equation of a profiled plate in (Dong *et al.* 2016a), where E^s, I_{11}, b, t, s and v^s are the elastic modulus, the second moment of the profiled cross-section about its neutral axis, width, thickness, arc length measured along the profiled cross section and Poisson's ratio of the skin sheet, respectively. For an even simpler case, if $D_{16} = D_{26} = 0, \frac{D_{12}+2D_{66}}{(D_{11}D_{22})^{1/2}} = 1$ and $D_{11} = D_{22} = D^s = \frac{E^s t^3}{12\left(1-v^{s2}\right)}$, Eq. (1) changes to the governing equation for an isotropic plate in (Ma *et al.* 2011), where D^s, E^s, t and v^s are the bending stiffness, Young's modulus, Poisson's ratio and thickness of the isotropic plate, respectively. The isotropic plate and the profiled plate are special cases of laminated plates from the view of mathematical modelling.

Assuming the following equations (Weaver and Nemeth 2007, Liu *et al.* 2014, Nemeth 1997)

$$\alpha = \left(\frac{D_{11}}{D_{22}}\right)^{1/4}; \quad \beta = \frac{D_{12}+2D_{66}}{(D_{11}D_{22})^{1/2}}; \quad \gamma = \frac{D_{16}}{(D_{11}^3 D_{22})^{1/4}}; \quad \delta = \frac{D_{26}}{(D_{11}D_{22}^3)^{1/4}}; \quad K = \frac{b^2 t \tau_{xy}}{\pi^2 (D_{11}D_{22}^3)^{1/4}} \tag{4}$$

Substituting Eqs. (2)-(4) into (1), yields

$$\alpha^2 w_{i,x_i x_i x_i x_i} + 2\beta w_{i,x_i x_i yy} + \frac{1}{\alpha^2} w_{i,yyyy} + 4\alpha\gamma w_{i,x_i x_i x_i y} + 4\delta \frac{1}{\alpha} w_{i,x_i yyy} + 2K \frac{1}{\alpha} \frac{\pi^2}{b^2} w_{i,x_i y} = q_i/(D_{11}D_{22})^{1/2} \quad |x_i| \le a_i/2 \tag{5}$$

Assuming $w_i(x_i, y) = f_i(\bar{x}_i) g(y)$, Eq. (3) may be written as

$$q_i(x_i, y) = -k_i w_i(x_i, y) = -k_i f_i(\bar{x}_i) g \tag{6}$$

where i = 1 and 2, g and f_i are the lateral direction and the longitudinal direction deflection function, respectively; k_i is the factor of stiffness, k_1 = 0 for non-contact areas and $k_2 \neq$ 0 for contact areas.

According to Fig. 1(d), $\bar{x}_i$ can be expressed as

$$\bar{x}_i = x_i + y \frac{1}{\tan\varphi} = x_i + y \cdot c \tag{7}$$

where φ is the skewed angle and $c = 1/\tan\varphi$ (Fig. 1(d)), it is noted that $\bar{x}_i = x_i - y \cdot c$ for the positive shear loading (See Appendix B), yields

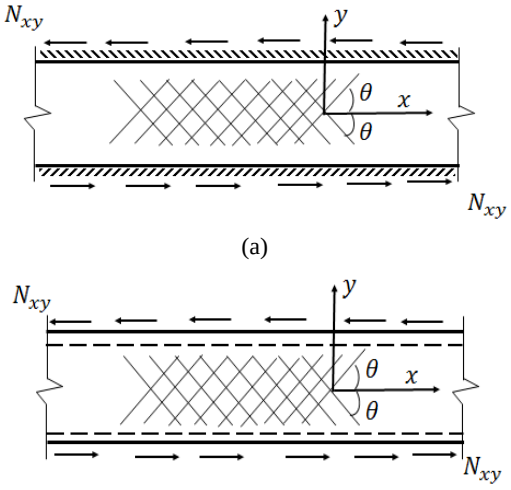

Fig. 2 Boundary conditions of the symmetrical laminated composite plate: (a) clamped edges; (b) simply supported edges

$$\left[\alpha^2 + 2\beta c^2 + \frac{1}{\alpha^2}c^4 + 4\alpha\gamma c + 4\frac{1}{\alpha}\delta c^3\right] f_i'''' g + \left[4\beta c + 4\frac{1}{\alpha^2}c^3 + 4\alpha\gamma + 12\frac{1}{\alpha}\delta c^2\right] f_i''' g' + \left[2\beta + 6\frac{1}{\alpha^2}c^2 + 12\frac{1}{\alpha}\delta c\right] f_i'' g'' + \left(4\frac{1}{\alpha^2}c + 4\frac{1}{\alpha}\delta\right) f_i' g''' + \frac{1}{\alpha^2} f_i g'''' + 2K\frac{1}{\alpha}\frac{\pi^2}{b^2}(c f_i'' g + f_i' g') + k_i f_i g \,/(D_{11}D_{22})^{1/2} = 0 \tag{8}$$

Consider the boundary conditions for Eq. (8) (Fig. 2), the lateral deflection function $g(y)$ can be assumed as (Ma *et al.* 2007, 2011, Jones and Milne 1976, Dalaei and Kerr 1995)

$$g(y) = \left[\frac{1}{4} - \left(\frac{y}{b}\right)^2\right]^2 \quad \text{for the clamped edges} \tag{9a}$$

$$g(y) = \cos\frac{\pi y}{b} \quad \text{for the simply supported edges} \tag{9b}$$

Multiplying the lateral deflection function $g(y)$ on both sides of Eq. (8) and taking the integral, yields:

For the laterally clamped edges

$$\left[\alpha^2 + 2\beta c^2 + \frac{1}{\alpha^2}c^4 + 4\alpha\gamma c + 4\frac{1}{\alpha}\delta c^3\right] f_i'''' - \frac{1}{b^2}\left(24\beta + 72\frac{1}{\alpha^2}c^2 + 144\frac{1}{\alpha}\delta c - 2\frac{1}{\alpha}c\pi^2 K\right) f_i'' + \frac{504}{b^4}\left(\frac{1}{\alpha^2} + \frac{b^4 k_i}{504(D_{11}D_{22})^{1/2}}\right) f_i = 0 \tag{10a}$$

For the laterally simply supported edges

$$\left[\alpha^2+2\beta c^2+\frac{1}{\alpha^2}c^4+4\alpha\gamma c+4\frac{1}{\alpha}\delta c^3\right]f_i''''-\frac{1}{b^2}\left(2\pi^2\beta+6\frac{1}{\alpha^2}c^2\pi^2+12\frac{1}{\alpha}\delta c\pi^2-2\frac{1}{\alpha}c\pi^2K\right)f_i''+\frac{\pi^4}{b^4}\left(\frac{1}{\alpha^2}+\frac{b^4k_i}{\pi^4(D_{11}D_{22})^{1/2}}\right)f_i=0 \quad (10b)$$

Assuming $f_i(\bar{x}_i)=\tilde{f}_i(\xi_i), \xi_i=\bar{x}_i/a_i, \phi_i=a_i/b$, $B_1=\left[\alpha^2+2\beta c^2+\frac{1}{\alpha^2}c^4+4\alpha\gamma c+4\frac{1}{\alpha}\delta c^3\right]$, $\tilde{k}_1=0$, we obtain

$$B_1\tilde{f}_i''''(\xi_i)-{\phi_i}^2B_2\tilde{f}_i''(\xi_i)+B_3{\phi_i}^4\tilde{f}_i(\xi_i)\left(\frac{1}{\alpha^2}+\tilde{k}_i\right)=0 \quad (11)$$

where $B_2=24\beta+72\frac{1}{\alpha^2}c^2+144\frac{1}{\alpha}\delta c-2\frac{1}{\alpha}c\pi^2K$, $B_3=504$, $\tilde{k}_2=k_r=\frac{b^4k_2}{504(D_{11}D_{22})^{1/2}}$, for a clamped edges; $B_2=2\pi^2\beta+6\frac{1}{\alpha^2}c^2\pi^2+12\frac{1}{\alpha}\delta c\pi^2-2\frac{1}{\alpha}c\pi^2K$, $B_3=\pi^4$, $\tilde{k}_2=k_r=\frac{b^4k_2}{\pi^4(D_{11}D_{22})^{1/2}}$ for a simply supported edges.

The lowest value of K is the shear buckling coefficient K_{cr}. The shear buckling coefficient Kcr can be obtained by using the continuous conditions between noncontact and contact areas and boundary conditions. The procedure of obtaining was illustrated in the previous studies (Ma *et al*. 2008b, 2011, Dong *et al*. 2016a, b). The general contact buckling solution of the laminated composite plate can be obtained based on Eq. (11).

3. Numerical examples and parametric study

In the present work, the material properties and ply thickness of the laminated composite plate are given as below unless noted otherwise. The laminated composite plate has the material property: longitudinal modulus E_{11} = 24.02 GPa; transverse modulus E_{22} = 3.42 GPa; shear modulus G_{12} = 2.17 GPa and Poisson's ratio ν_{12} = 0.35 (Awad *et al*. 2014). Each ply thickness is 0.125 mm.

ABAQUS was used to simulate the buckling behaviour of the laminated composite plates. In the current study, l = 2000 mm (plate length) and b = 200 mm (plate width), so the aspect ratio of the composite plate is 10. The ratio of width to thickness of laminated plate is chosen to be no less than 100 in order to minimize the effects of transverse shear. The laminated composite plate was represented as S8R elements. The tensionless elastic Winkler foundation was represented as springs in the FE analysis.

3.1 Convergence study of FE analysis mesh

To determine the appropriate mesh size of the FE model, a convergence study was conducted and the analysis results are presented in Table 1. An orthotropic plate without foundation (unrestrained plate) and with the following stacking sequence $[0°/90°/0°/90°]_s$ was considered as one example to analyse for the convergence study. The configuration of the desktop computer used was: Intel Core i5-4590, 2 cores, 3.3 GHz, maximum memory 8 GB. From Table 1, the error reduces and calculation time increases as mesh size decreases, in other words, more accurate results of FE analysis can be obtained for the plate with more elements, which is obviously as expected. However, the more elements we have, the more calculation time the model takes. Both elements S4R and S8R were analysed in the convergence study (Table 1). For element S8R with mesh size 2 mm × 2 mm, the computer could not carry on the calculation because the memory allocation for calculation exceeded the memory in the current desktop. Based on the result of convergence analysis, with the

Table 1 Result of convergence analysis

Boundary condition	K_{cr} Anal.	FE method						
		Mesh size (mm)	Element S4R			Element S8R		
			K_{cr}	vs. anal. %	Time (s)	K_{cr}	vs. anal. %	Time (s)
Clamped	7.39	20×20	8.28	11.95	17	7.43	0.44	30
	7.39	10×10	7.61	2.98	31	7.53	1.87	99
	7.39	8×8	7.54	1.99	38	7.41	0.28	180
	7.39	5×5	7.46	0.93	92	7.41	0.27	468
	7.39	4×4	7.44	0.69	170	7.41	0.27	829
	7.39	2×2	7.42	0.37	1337	-	-	*
Simply supported	4.33	20×20	4.51	4.16	13	4.26	1.69	26
	4.33	10×10	4.32	0.34	27	4.25	1.75	79
	4.33	8×8	4.29	0.85	34	4.25	1.75	107
	4.33	5×5	4.27	1.42	77	4.25	1.77	286
	4.33	4×4	4.26	1.56	119	4.25	1.78	387
	4.33	2×2	4.25	1.75	502	-	-	*

*Note The memory allocation exceeds 8 GB in the current desktop

Table 2 Flexural stiffness and parameter β for different lay-up sequence

Laminated scheme	D_{11} (Nmm)	D_{12} (Nmm)	D_{22} (Nmm)	D_{66} (Nmm)	β
$[0°/90°]_s$	227.60	13.07	63.62	22.70	0.49
$[(0°/90°)2]_s$	1492.85	104.53	836.95	181.22	0.42
$[(0°/90°)3]_s$	4669.44	352.79	3193.66	611.61	0.41

accuracy and time cost taken into account, the element S8R and mesh size 10 mm × 10 mm was chosen in the FE model for all FE analysis in this study.

3.2 Orthotropic plate under in-plane shear

In order to verify the effect of the lay-up sequence of composite materials on the shear critical stress, three combinations of the composite layers were considered, i.e.,

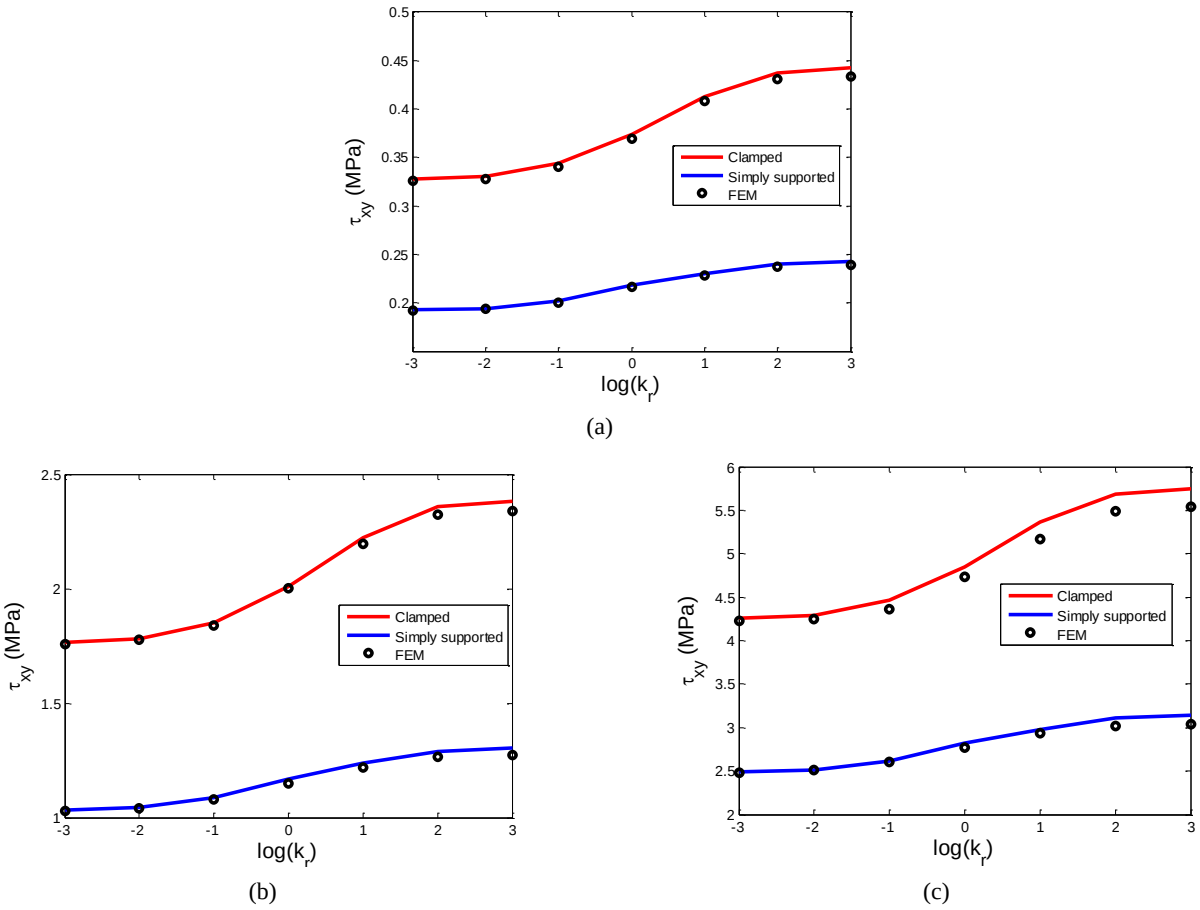

Fig. 3 Critical shear stress load for different k_r: (a) $[0°/90°]_s$; (b) $[(0°/90°)2]_s$; (c) $[(0°/90°)3]_s$

Table 3 Negative shear critical buckling coefficient K_{cr} for different symmetrical angles under foundation stiffness factor k_r = 1

$[\pm\theta]_s$	β	γ	δ	K_{cr} for clamped			K_{cr} for simply supported		
				Analytical	FE method	Difference %	Analytical	FE method	Difference %
0°	0.61	0.00	0.00	9.02	8.93	-0.95	5.29	5.25	-0.74
10°	0.77	0.16	0.06	10.63	10.61	-0.28	6.23	6.20	-0.48
20°	1.17	0.30	0.16	13.21	12.91	-2.27	7.82	7.75	-0.92
30°	1.58	0.39	0.28	15.45	15.07	-2.45	9.38	9.14	-2.59
40°	1.82	0.41	0.38	17.41	16.95	-2.65	10.32	10.05	-2.59
45°	1.86	0.40	0.40	17.74	17.18	-3.14	10.49	10.19	-2.79
50°	1.82	0.38	0.41	17.73	17.09	-3.57	10.45	10.14	-3.00
60°	1.58	0.28	0.39	16.45	15.73	-4.39	9.77	9.48	-2.94
70°	1.17	0.16	0.30	14.09	13.61	-3.44	8.34	8.05	-3.50
80°	0.77	0.06	0.16	11.31	10.75	-4.97	6.58	6.34	-3.60
90°	0.61	0.00	0.00	9.02	8.618	-4.41	5.29	5.11	-3.28

Table 4 Positive shear critical buckling coefficient K_{cr} for different symmetrical angles under foundation stiffness factor k_r = 1

$[\pm\theta]_s$	β	γ	δ	K_{cr} for clamped			K_{cr} for simply supported		
				Analytical	FE	Difference %	Analytical	FE	Difference %
0°	0.61	0.00	0.00	9.02	8.93	-0.95	5.29	5.25	-0.74
10°	0.77	0.16	0.06	8.26	8.27	0.18	4.93	4.85	-1.59
20°	1.17	0.30	0.16	7.88	7.86	-0.29	4.81	4.72	-1.92
30°	1.58	0.39	0.28	7.50	7.45	-0.66	4.59	4.50	-2.10
40°	1.82	0.41	0.38	7.40	7.29	-1.41	4.43	4.30	-2.83
45°	1.86	0.40	0.40	7.24	7.05	-2.63	4.29	4.16	-3.04
50°	1.82	0.38	0.41	7.24	7.03	-2.94	4.15	3.99	-3.78
60°	1.58	0.28	0.39	7.02	6.77	-3.48	3.98	3.83	-3.77
70°	1.17	0.16	0.30	7.02	6.77	-3.45	3.95	3.78	-4.27
80°	0.77	0.06	0.16	7.47	7.20	-3.60	4.40	4.18	-4.90
90°	0.61	0.00	0.00	9.02	8.62	-4.41	5.29	5.07	-4.16

[0°/90°]s, [0°/90°/0°/90°]s and [0°/90°/0°/90°/0°/90°]$_s$. Based on the classical lamination plate theory (Jones 1998 and Reddy 2004), the plate flexural stiffness D_{11}, D_{12}, D_{22} and D_{66} can be calculated, and $\beta = \frac{D_{12}+2D_{66}}{(D_{11}D_{22})^{1/2}}$, leading to the calculation results shown in Table 2.

Based on Eq. (4), $\tau_{xy} = \frac{K_{cr}\pi^2(D_{11}D_{22}^3)^{1/4}}{b^2t}$. As shown in Fig. 3, the analytical results of the three lay-up sequences are presented for both simply supported and clamped edges. To validate the analytical solution, the FE analysis was conducted and the corresponding results were shown in Fig. 3 as well. From Fig. 3, it can be observed that a good agreement was reached. It can also be seen that the number of layers have great influence on the shear critical stress. For the same ply thickness, the more layers, the larger the shear critical stress. In other words, the shear critical stress increases with increasing plate thickness.

3.3 Anisotropic plate under in-plane shear

In this section, the effects of D_{16} and D_{26} are taken into account, i.e., anisotropic parameters γ and δ are not equal to zero. Eleven types of laminated composite lay-up

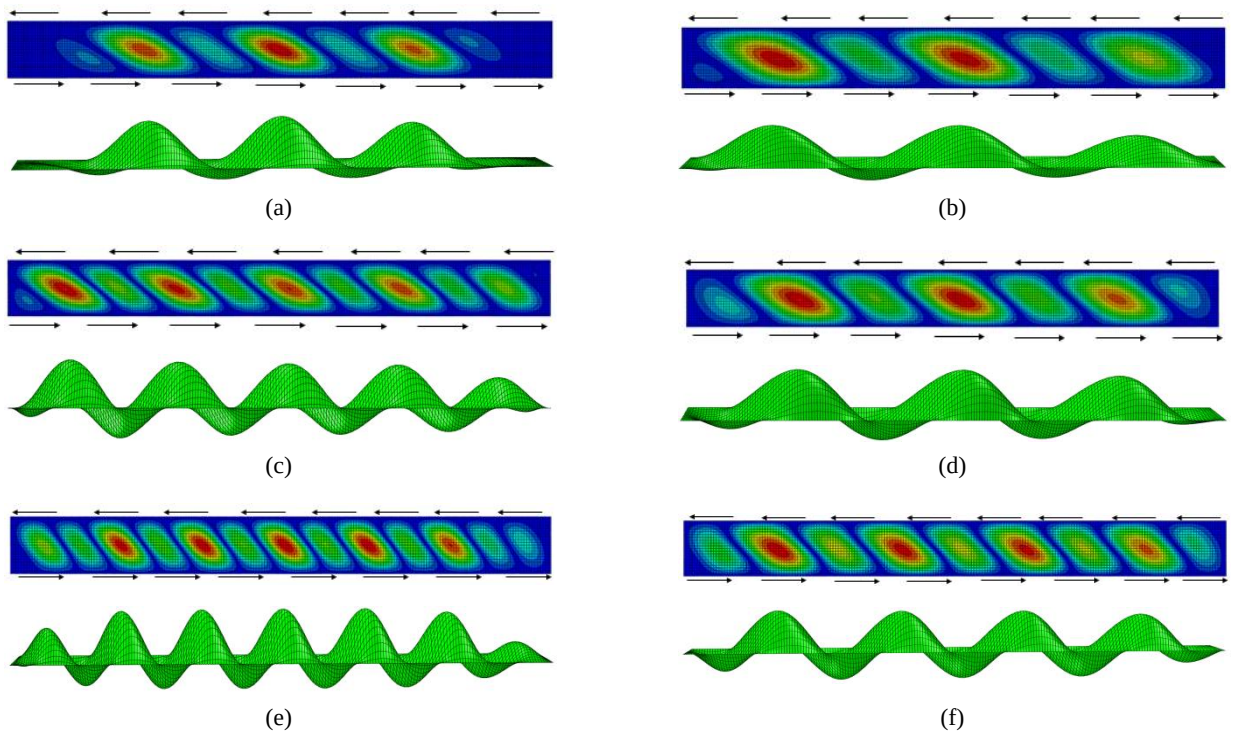

Fig. 4 Buckling mode of FE method under negative shear for $k_r = 1$: (a) ply angle 30° with clamped edges; (b) ply angle 30° with simply supported edges; (c) ply angle 45° with clamped edges; (d) ply angle 45° with simply supported edges; (e) ply angle 60° with clamped edges; (f) ply angle 60° with simply supported edges

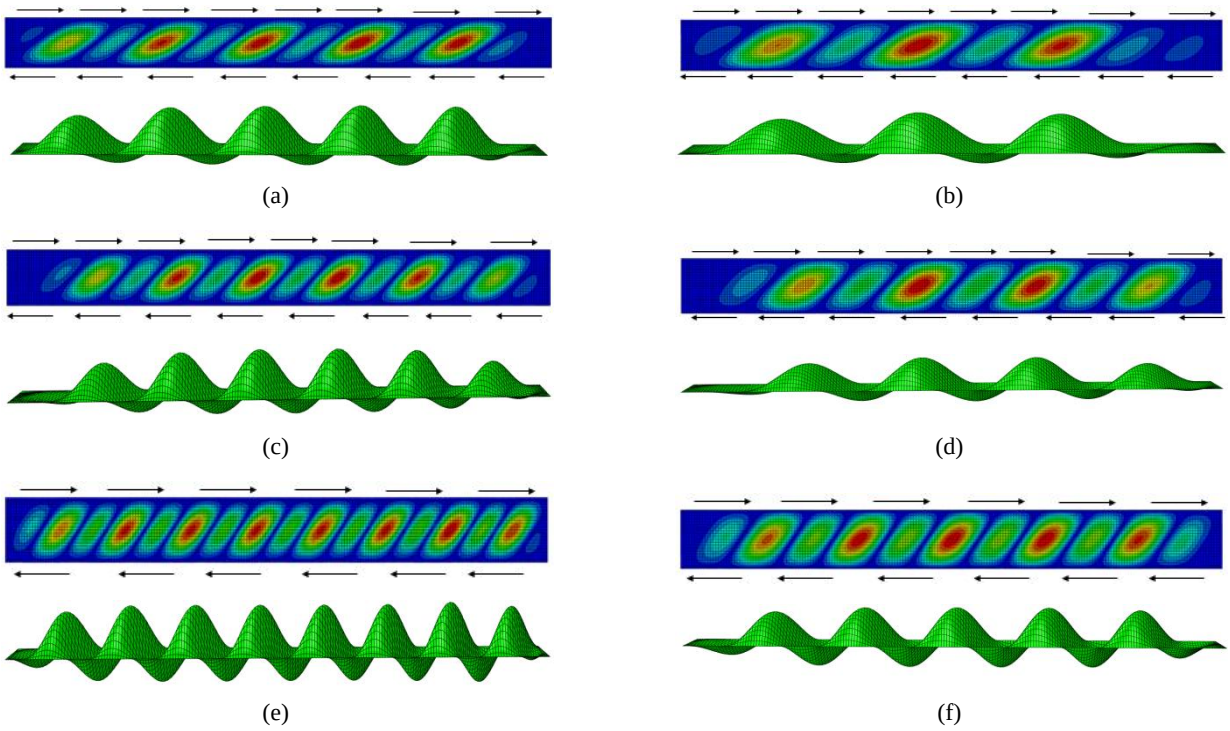

Fig. 5 Buckling mode of FE method under positive shear for $k_r = 1$: (a) ply angle 30° with clamped edges; (b) ply angle 30° with simply supported edges; (c) ply angle 45° with clamped edges; (d) ply angle 45° with simply supported edges; (e) ply angle 60° with clamped edges; (f) ply angle 60° with simply supported edges

sequences were used to analyze the effect of ply angle on the shear critical buckling coefficient K_{cr} and seven types of foundation stiffness factors were used. For the orthotropic plate, the shear critical buckling coefficient K_{cr} is the same for the in-plane negative and positive shear loading. However, for the anisotropic plate, the shear critical buckling coefficient K_{cr} will be different for the in-plane negative and positive shear loading. In fact, the shear critical buckling coefficient K_{cr} of positive loading is smaller than that of negative loading.

When the foundation stiffness k_r = 1, Tables 3 and 4 give the calculation results of the orthotropic parameter β, anisotropic parameters (γ and δ) and the shear critical buckling coefficient K_{cr} under negative and positive in-plane shear loading, respectively. To study the influence of edge conditions on shear critical buckling coefficient of laminated composite plate on the elastic tensionless foundation, the results in Tables 3 and 4 include both simply supported and clamped edges. To verify the analytical solution, the results of the FE analysis are also presented in Tables 3 and 4. From Tables 3 and 4, it is clearly observed that the maximum error between the analytical solution and FE analysis result is smaller than 5%. For the anisotropic plate under positive shear loading, the maximum value of the shear critical buckling coefficient K_{cr} occurs at 0° and 90°, and the minimum value occurs at angle between 60° and 70°. While for the anisotropic plate under negative shear loading, the maximum value of the shear critical buckling coefficient K_{cr} occurs at angle between 45° and 50°, and the minimum value occurs at angle of 0° and 90°.

The buckling modes of the FE analysis of the anisotropic plate for k_r = 1 under negative and positive in-plane shear loading are presented in Figs. 4 and 5, respectively. To analyze the influence of the edge conditions on the shear critical buckling coefficient of an anisotropic plate restrained on an elastic tensionless foundation, both clamped and simply supported edge conditions were taken into account, with the results given in Figs. 4 and 5. As seen from Figs. 4 and 5, compared with clamped boundary condition, the number of buckling half waves with simply supported tends to have lesser half waves at the same conditions, like ply angle and foundation stiffness parameter. The number of the buckling half waves increases with the increase of ply angle θ. Namely, the buckling modes of the anisotropic plates with bigger ply angle θ tend to have more half waves than those with smaller ply angle θ. For a specific ply angle θ, the anisotropic plates under in-plane positive shear loading tend to have more buckling half waves than those under in-plane negative shear loading. In other words, if the ply angle θ is same, one single outward buckling half wavelength of the anisotropic plates under in-plane negative shear loading will be longer than that under in-plane positive shear loading.

In order to highlight the effect of ply angle and foundation stiffness on the critical shear buckling coefficient K_{cr}, the critical shear buckling coefficient K_{cr} versus the ply angle θ and the critical shear buckling coefficient K_{cr} versus foundation stiffness k_r are plotted in Figs. 6 and 7, respectively. As expected, the critical shear buckling coefficient K_{cr} rises with the increase of foundation stiffness k_r. Both clamped and simply supported conditions are presented in Figs. 6 and 7. As depicted, the critical shear buckling coefficient K_{cr} with clamped edges is larger than that with simply supported edges. For the ply

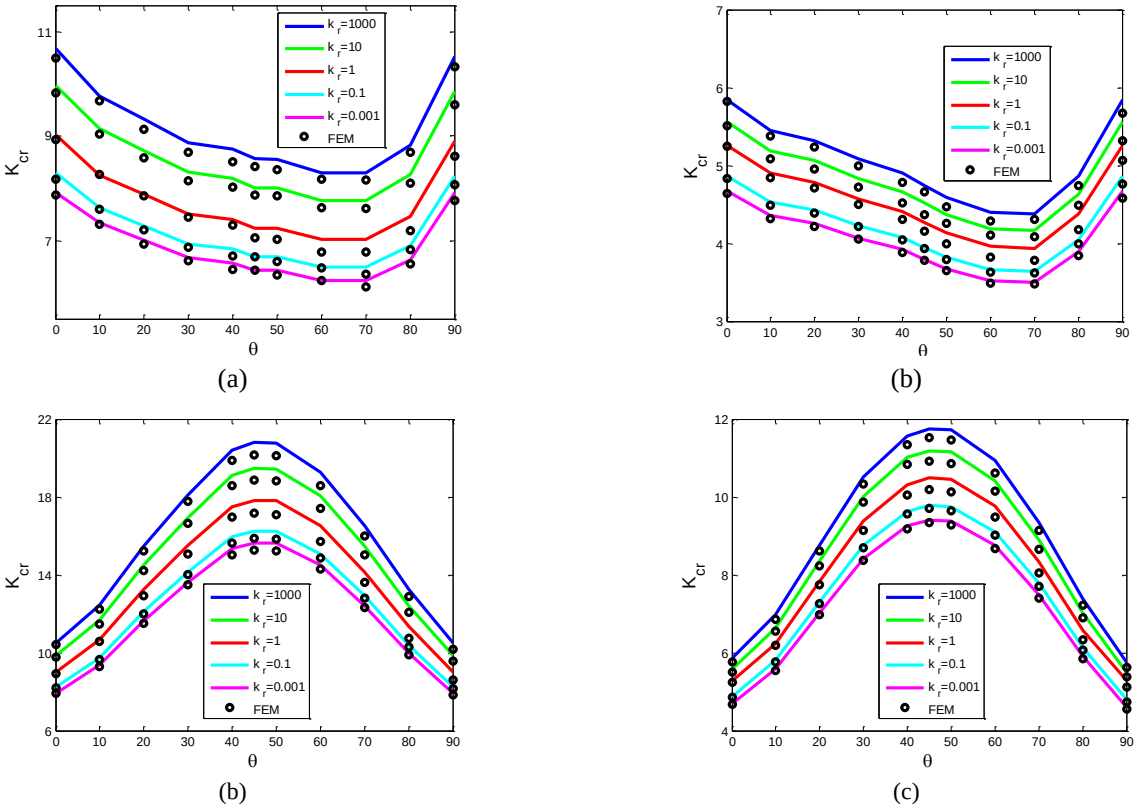

Fig. 6 Shear buckling coefficients versus $[\pm\theta]_s$: (a) clamped edges under positive shear; (b) simply supported edges under positive shear; (c) clamped edges under negative shear; (d) simply supported edges under negative shear

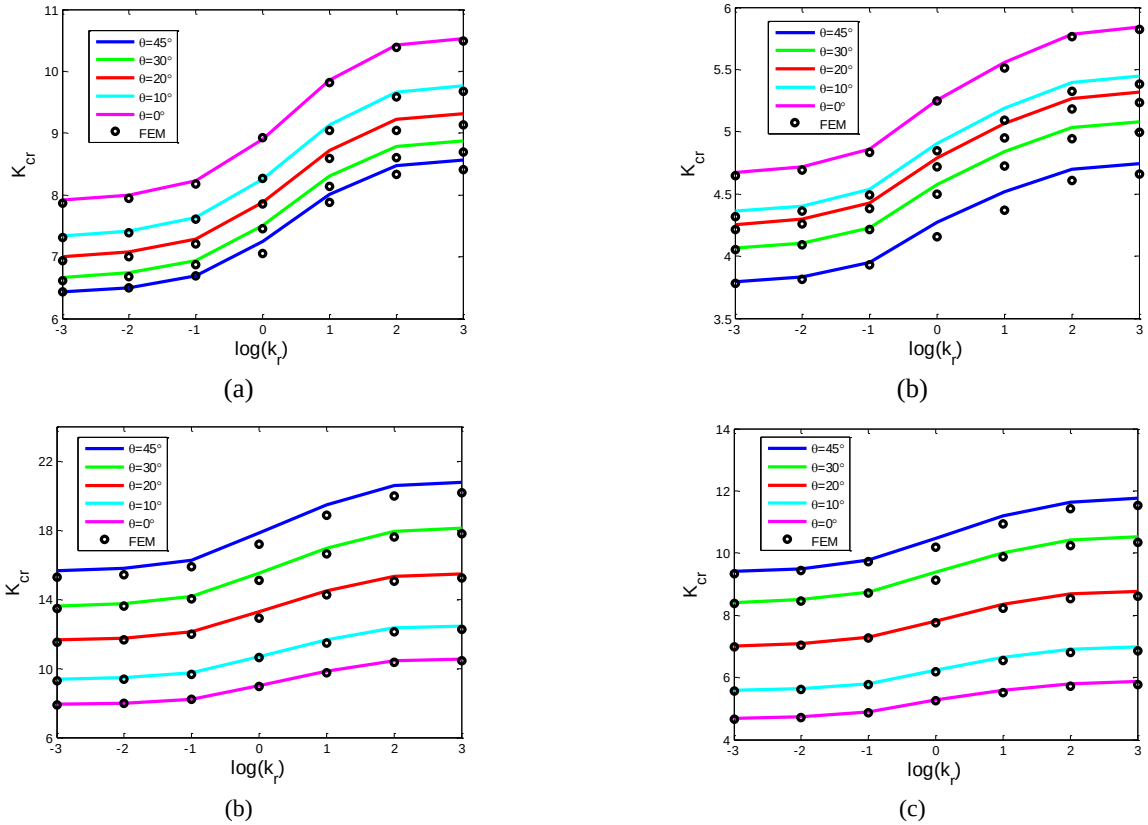

Fig. 7 Shear critical buckling coefficient K_{cr} versus foundation stiffness k_r: (a) clamped edges under positive shear; (b) simply supported edges under positive shear; (c) clamped edges under negative shear; (d) simply supported edges under negative shear

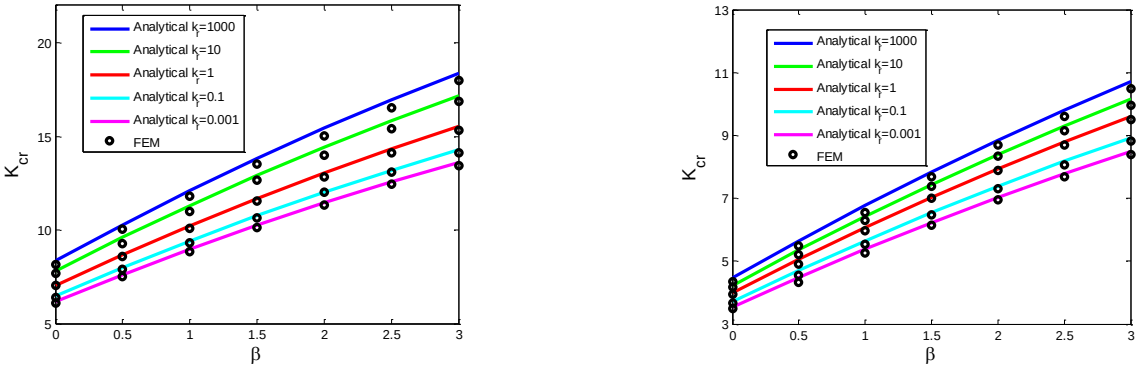

Fig. 8 Shear critical buckling coefficient K_{cr} versus orthotropic parameter β for different k_r: (a) clamped edges plate; (b) simply supported edges plate

angle range between 0° and 45°, Fig. 7 shows that the critical shear buckling coefficient K_{cr} of the anisotropic plate decreases under positive shear loading and increases under negative shear loading with the increase of ply angle. In addition, to verify the analytical solutions, the results of the FE analysis were plotted in Figs. 6 and 7. From Figs. 6 and 7, it could be observed that a good agreement was obtained between the FE analysis and analytical solution.

3.4 Effect of orthotropic parameters (α and β) and anisotropic parameters (δ and γ)

The orthotropic parameters (α and β) and anisotropic parameters (δ and γ) are defined in Eq. (4). If D_{16} and D_{26} are not taken into account, i.e., $D_{16} = 0$, $D_{26} = 0$, the orthotropic laminated composite plate may be obtained. For infinitely laminated composite plates, the shear contact buckling coefficient is independent of the orthotropic parameter α (Nemeth 1992, 1997, Liu *et al*. 2014, Weaver and Nemeth 2007). Thus, the shear buckling coefficient of the orthotropic plates is only expressed by the orthotropic parameter β (Fig. 8). Fig. 8 illustrates that the shear critical buckling coefficient K_{cr} may increase with increase of foundation stiffness k_r for a specific value of orthotropic parameter β. In addition, for a specific value of k_r, the shear critical buckling coefficient K_{cr} may rise, caused by an increase of orthotropic parameter β. Additionally, for a specific value of k_r and orthotropic parameter β compared with simply supported, the shear critical buckling coefficient K_{cr} of a plate with clamped is bigger.

However, if D_{16} and D_{26} are considered, i.e., $D_{16} \neq 0$, $D_{26} \neq 0$, the anisotropic laminated composite plate is obtained. The solutions of shear contact buckling coefficient for the anisotropic laminated composite plate are more complicated than those of the orthotropic plates. Besides the orthotropic parameter β, more parameters have to be considered for anisotropic laminated composite material, namely the anisotropic parameters (γ and δ).

To further study the effect of anisotropic parameters (γ and δ) on the shear buckling coefficient for the anisotropic laminated composite plate on elastic foundation, one more example is given here. Consider that the thickness of the plate is constant and the number of layers increases until the shear buckling coefficient reaches the value of the orthotropic laminated composite plate. In the present example, the thickness of the plate is 0.5 mm, the lay-up sequences are $[45°/-45°]_s$, $[45°/-45°/45°/-45°]_s$, $[45°/-45°/45°/-45°/45°/-45°]_s$, $[45°/-45°/45°/-45°\ldots]_s$, …, $[(45°/-45)_\infty]_s$ and the foundation stiffness $k_r = 1$. Based on the CLT (Jones 1998, Reddy 2004), the plate flexural stiffness D_{11}, D_{12}, D_{16}, D_{22}, D_{26} and D_{66} can be calculated, and using Eq. (4) the corresponding orthotropic parameter β and anisotropic parameters (γ and δ) may be calculated, with the calculation results given in Table 5. The results of the shear buckling coefficient were obtained and plotted in Fig. 9, and the results of the corresponding FE analysis are shown in Fig. 9 as well.

Again, for the laminated composite plate resting on a tensionless elastic foundation, to highlight the influence of edge conditions on the local buckling, two edge conditions are given in this example, i.e., clamped and simply supported edge conditions. Fig. 9 shows that the shear buckling coefficient of the anisotropic plate tends to the value of the orthotropic plate. The phenomenon also occurs for the finite laminated composite plate (Chen and Qiao 2015). When the anisotropic plate is subjected to a positive shear force, the shear buckling coefficient increases with the decrease of anisotropic parameters $\gamma = \delta \neq 0$, until it reaches the value of the orthotropic plate, i.e., the anisotropic parameters $\gamma = \delta = 0$. If the anisotropic plate is subjected to a negative shear force, the shear buckling coefficient decreases with the decrease of anisotropic parameters $\gamma = \delta \neq 0$, until it reaches the value of the orthotropic plate if the anisotropic parameters $\delta = \gamma = 0$. Fig. 9 demonstrates that this curve of shear buckling coefficient versus $\gamma = \delta$ varies approximately linearly. That means that the shear buckling coefficient can decrease or increase with the increase of the number of layers for negative or positive shear loading, respectively, until the shear buckling coefficients reach to the value of the orthotropic plate.

Weaver and Nemeth presented the coupled dependence of the anisotropic parameters γ and δ for nine different laminated composite materials (Weaver and Nemeth 2007). Fig. 10 gives the relationship between γ and δ on ply angle θ for the symmetrical $[\pm\theta]_s$ laminated composite plates. The mathematical relationship between anisotropic parameters γ

Table 5 Flexural stiffness and other parameters for different lay-up sequences

Laminated scheme	D_{11} (Nmm)	D_{12} (Nmm)	D_{16} (Nmm)	D_{22} (Nmm)	D_{26} (Nmm)	D_{66} (Nmm)	β	γ	δ
$[45°/-45°]_s$	101.99	56.69	40.99	101.99	40.99	66.27	1.86	0.40	0.40
$[(45°/-45°)2]_s$	101.99	56.69	20.50	101.99	20.50	66.27	1.86	0.20	0.20
$[(45°/-45°)3]_s$	101.99	56.69	12.15	101.99	12.15	66.27	1.86	0.12	0.12
$[(45°/-45°)4]_s$	101.99	56.69	10.25	101.99	10.25	66.27	1.86	0.10	0.10
$[(45°/-45°)\infty]_s$ (orthotropic)	101.99	56.69	0.00	101.99	0.00	66.27	1.86	0.00	0.00

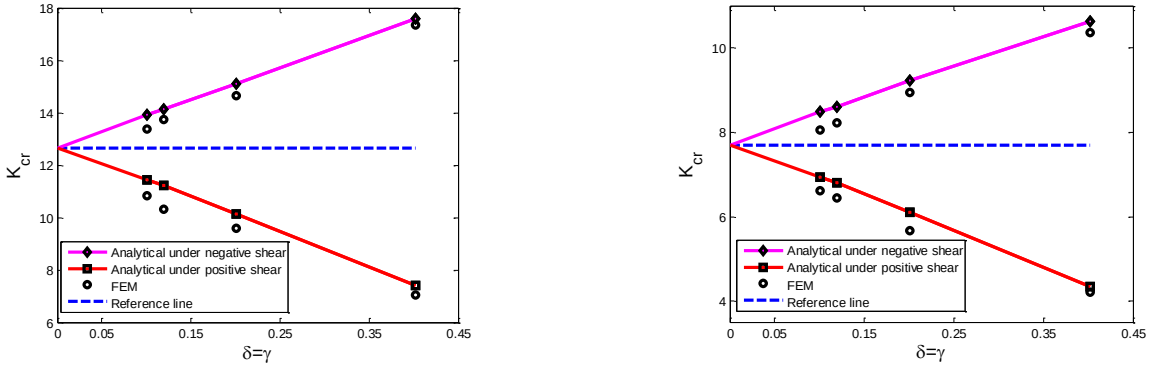

(a) (b)

Fig. 9 Shear critical buckling coefficient under k_r = 1: (a) clamped; and (b) simply supported

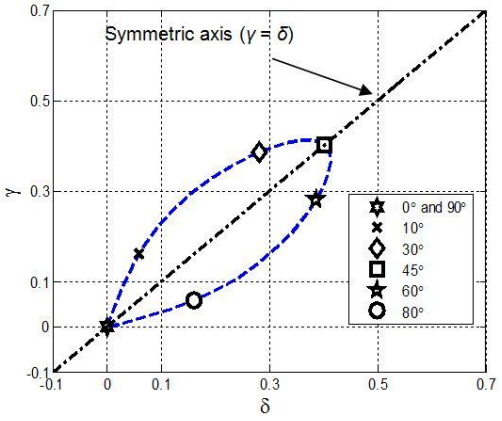

Fig. 10 Relationship between anisotropic parameters γ and δ for symmetrical $[\pm\theta]_s$

and δ also can be found. The function (γ and δ) on the top of the symmetric axis ($\gamma = \delta$) may be defined as the inverse of the function (γ and δ) on the bottom of the symmetric axis ($\gamma = \delta$). For example, for anisotropic parameters for θ=30° on the bottom of the symmetric axis ($\gamma = \delta$), the anisotropic parameters may be expressed as [δ_{30}, γ_{30}], and if θ = 60°, the anisotropic parameters on the top of the symmetric axis may be expressed as [δ_{60}, γ_{60}], thus $\delta_{30} = \gamma_{60}$ and $\gamma_{30} = \delta_{60}$.

4. An example

Consider an orthotropic clamped plate resting on a tensionless elastic foundation under uniform in-plane shear

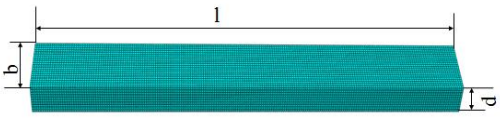

Fig. 11 Geometry of the foundation

loading. The dimension of the orthotropic plate is b = 200 mm, l = 2000 mm, t = 1 mm. The material properties of the orthotropic plate are same as Section 3. The material property of the foundation is assumed as an isotropic elastic material in this study. The elastic modulus of the foundation material, $\nu^f = 0.2$ and E^f varies between 3.93 × 10-05 MPa and 39.27 MPa (i.e., E^f is 3.93 × 10-05 MPa, 3.93 × 10-04 MPa, 3.93 × 10-03 MPa, 3.93 × 10-02 MPa, 3.93 × 10-01 MPa, 3.93 MPa and 39.27 MPa, respectively). The relevant foundation dimensional parameters are: b = 200 mm, l = 2000 mm and d = 100 mm (Fig. 11).

For the clamped plate, the effective foundation stiffness can be calculated as $\tilde{k}_2 = k_r = \frac{b^4 k_2}{504(D_{11}D_{22})^{1/2}}$. $k_2 = \frac{E^f}{b \times d_0^f}$, the non-dimensional factor d_0^f is related to d/b and ν^f (Ma *et al.* 2008b), $d_0^f = 0.81$ in this example, so $k_r = \frac{b^3}{504(D_{11}D_{22})^{1/2}} \frac{E^f}{d_0^f}$ can be approximately calculated. The critical shear stress can be calculated by $\tau_{xy} = \frac{K_{cr}\pi^2 (D_{11}D_{22}^3)^{1/4}}{b^2 t}$, the result is shown in Fig. 12. Thus, the relationship between foundation stiffness factor k_r versus the critical shear stress τ_{xy} may be plotted in Fig. 12. The curve also illustrates the relationship between elastic

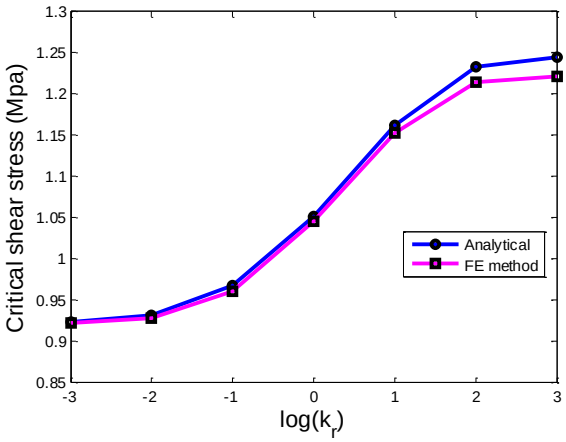

Fig. 12 Critical shear stress load of the orthotropic plate

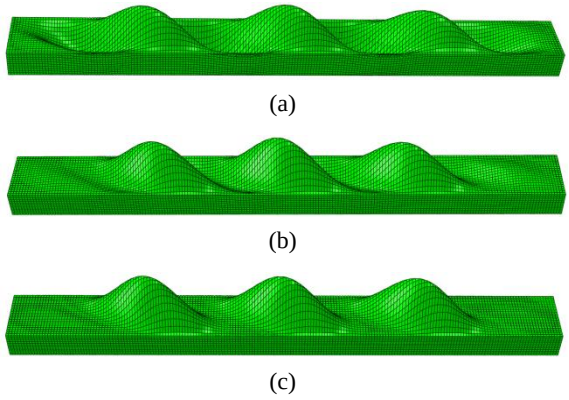

Fig. 13 Buckling mode of FE method for an orthotropic plate: (a) orthotropic plate with $k_r = 0.001$; (b) $k_r = 1$; (c) $k_r = 1000$

modulus of the foundation material versus the critical shear stress.

According to the above analysis, a FE model was created to validate the method of the proposed solution in the current example. The critical shear stresses of the FE method versus the foundation stiffness are plotted in Fig. 12 and the buckling modes from FE method are presented in Fig. 13. From Fig. 12, it is clearly seen that a good agreement can be observed between the critical shear stress of the FE simulation and the analytical result. In addition, Fig. 13 demonstrates that the sizes of inward buckling half waves of the orthotropic plate become smaller than those of outward half waves with the increase of the stiffness factor of foundation. When the foundation stiffness parameter k_r = 0.001, the length of inward and outward half waves are nearly the same. While for foundation stiffness parameter k_r = 1000, there are only outward half waves left and there are no inward half waves. This phenomenon accords with the previous studies (Ma *et al*. 2008b, Dong *et al*. 2016a, b). Thus, it illustrates that it is effective and feasible to analyze the contact buckling of composite plates using the proposed method.

5. Conclusions

A numerical simulation procedure for predicting directional typhoon wind fields over complex terrain has been proposed in this study.

This study has investigated the local buckling analysis of solution. Based on these analyses, conclusions co infinite thin rectangular symmetrically laminated composite plates restrained by tensionless elastic founda-tions under uniform in-plane shear loading. To derive the analytical solution of the contact buckling coefficient, a one-dimensional mathematical method was applied. Parametric studies and numerical examples were carried out to study the effect of the foundation stiffness and ply angle on the critical buckling loads. A series of FE analyses were conducted to verify the analytical solution of the examples in the parametric study, and the FE analysis result was in accordance with analytical uld be drawn as follows:

- The value of the shear critical buckling coefficient K_{cr} with simply supported edges is smaller than that with clamped edges.
- Compared with simply supported, the laminated composite clamped plates are inclined to have more half waves.
- The buckling modes of the laminated composite plates with bigger ply angle θ tend to have more half waves than those with smaller ply angle θ.
- The shear critical buckling coefficient K_{cr} of orthotropic plate is the same for the negative and positive shear loading. However, the shear critical buckling coefficient K_{cr} of anisotropic plate under positive shear loading tends to be smaller than that under negative shear loading.
- For a specific ply angle θ, the anisotropic plates under in-plane positive shear loading tend to have more buckling half waves than those under in-plane negative shear loading.
- For symmetrical $[\pm\theta]_s$ laminated composite plates, the anisotropic parameters λ and δ may be expressed as a symmetric relationship about $\gamma = \delta$. This means that the function (λ and δ) on the top of the symmetric axis ($\gamma = \delta$) may be defined as the inverse function of the function (γ and δ) on the bottom of the symmetric axis ($\gamma = \delta$).
- In general, the critical shear buckling coefficient K_{cr} increases with the increase of the foundation stiffness k_r.

References

Altunsaray, E. and Bayer, I. (2014), "Buckling of symmetrically laminated quasi-isotropic thin rectangular plates", *Steel Compos. Struct., Int. J.*, **17**(3), 305-320.

Arabzade, A., Moharami, H. and Ayazi, A. (2011), "Local elastic buckling coefficients of steel plates in composite steel plate shear walls", *Scientia Iranica*, **18**(1), 9-15.

Ashour, A.S. (2003), "Buckling and vibration of symmetric laminated composite plates with edges elastically restrained", *Steel Compos. Struct., Int. J.*, **3**(6), 439-450.

Awad, Z.K., Aravinthan, T. and Zhuge, Y. (2014), "Finite element analysis of glass fibre reinforced polymer single and glue

laminated sandwich beams under four point bending", *Res. Civil Environ. Eng.*, **2**(1), 24-44.
Baseri, V., Jafari, G.S. and Kolahchi, R. (2016), "Analytical solution for buckling of embedded laminated plates based on higher order shear deformation plate theory", *Steel Compos. Struct., Int. J.*, **21**(4), 883-919.
Becheri, T., Amara, K., Bouazza, M. and Benseddiq, N. (2016). "Buckling of symmetrically laminated plates using nth-order shear deformation theory with curvature effects", *Steel Compos. Struct., Int. J.*, **21**(6), 1347-1368.
Bradford, M.A., Smith, S.T. and Oehlers, D.J. (2000), "Semi-compact steel plates with unilateral restraint subjected to bending, compression and shear", *J. Constr. Steel Res.*, **56**(1), 47-67.
Chen, Q. and Qiao, P. (2015), "Shear buckling of rotationally-restrained composite laminated plates", *Thin-Wall. Struct.*, **94**, 147-154.
Dalaei, M. and Kerr, A.D. (1995), "Analysis of clamped rectangular orthotropic plates subjected to a uniform lateral load", *Int. J. Mech. Sci.*, **37**(5), 527-535.
Darvizeh, M., Darvizeh, A. and Sharma, C. (2002), "Buckling analysis of composite plates using differential quadrature method (DQM)", *Steel Compos. Struct., Int. J.*, **2**(2), 99-112.
Dong, J., Zhuge, Y., Mills, J.E. and Ma, X. (2016a), "Local buckling of profiled skin sheets resting on tensionless elastic foundations under in-plane shear loading", *Eur. J. Mech. A: Solids*, **58**, 131-139.
Dong, J., Zhuge, Y., Mills, J.E. and Ma, X. (2016b), "Local buckling of profiled skin sheets resting on tensionless elastic foundations under uniaxial compression", *Thin-Wall. Struct.*, **103**, 81-89.
Jones, R.M. (1998), *Mechanics of Composite Materials*, CRC Press.
Jones, R. and Milne, B.J. (1976), "Application of the extended Kantorovich method to the vibration of clamped rectangular plates", *J. Sound Vib.*, **45**(3), 309-316.
Keage, N., Maiolo, C., Pierotti, R. and Ma, X. (2011), "Experimental study and numerical simulation on compressive buckling behavior of thin steel skins in unilateral contact with rigid constraints", *Front. Archit. Civil Eng. China*, **5**(3), 335-343.
Khalili, S., Abbaspour, P. and Fard, K.M. (2013), "Buckling of non-ideal simply supported laminated plate on Pasternak foundation", *Appl. Math. Comput.*, **219**(12), 6420-6430.
Kosteletos, S. (1992), "Shear buckling response of laminated plates", *Compos. Struct.*, **20**(3), 147-154.
Leissa, A. (1983), "Buckling of composite plates", *Compos. Struct.*, **1**(1), 51-66.
Li, D., Smith, S. and Ma, X. (2016), "End condition effect on initial buckling performance of thin plates resting on tensionless elastic or rigid foundations", *Int. J. Mech. Sci.*, **105**, 83-89.
Liu, Q., Qiao, P. and Guo, X. (2014), "Buckling analysis of restrained orthotropic plates under combined in-plane shear and axial loads and its application to web local buckling", *Compos. Struct.*, **111**, 540-552.
Ma, X., Butterworth, J.W. and Clifton, C. (2007), "Compressive buckling analysis of plates in unilateral contact", *Int. J. Solids Struct.*, **44**(9), 2852-2862.
Ma, X., Butterworth, J.W. and Clifton, G.C. (2008a), "Initial compressive buckling of clamped plates resting on tensionless elastic or rigid foundations", *J. Eng. Mech.*, **134**(6), 514-518.
Ma, X., Butterworth, J.W. and Clifton, G.C. (2008b), "Practical analysis procedure for compressive local buckling of skin sheets in composite panels", *Int. J. Adv. Steel Constr.*, **4**(3), 230-242.
Ma, X., Butterworth, J.W. and Clifton, G.C. (2008c), "Unilateral contact buckling of lightly profiled skin sheets under compressive or shearing loads", *Int. J. Solids Struct.*, **45**(3-4), 840-849.
Ma, X., Butterworth, J.W. and Clifton, G.C. (2011), "Shear buckling of infinite plates resting on tensionless elastic foundations", *Eur. J. Mech. A: Solids*, **30**(6), 1024-1027.
Muradova, A.D. and Stavroulakis, G.E. (2012), "Buckling and postbuckling analysis of rectangular plates resting on elastic foundations with the use of the spectral method", *Comput. Methods Appl. Mech. Eng.*, **205-208**, 213-220.
Nemeth, M.P. (1992), "Buckling behavior of long symmetrically laminated plates subjected to combined loadings", NASA TP-3195.
Nemeth, M.P. (1997), "Buckling behavior of long symmetrically laminated plates subjected to shear and linearly varying axial edge loads", NASA TP-3659.
Paliwal, D. and Ghosh, S.K. (2000), "Stability of orthotropic plates on a Kerr foundation", *AIAA J.*, **38**(10), 1994-1997.
Panahandeh-Shahraki, D., Mirdamadi, H.R. and Shahidi, A.R. (2013), "Nonlinear buckling analysis of laminated composite curved panels constrained by Winkler tensionless foundation", *Eur. J. Mech. A: Solids*, **39**, 120-133.
Qiao, P. and Huo, X. (2011), "Explicit local buckling analysis of rotationally-restrained orthotropic plates under uniform shear", *Compos. Struct.*, **93**(11), 2785-2794.
Reddy, J.N. (2004), *Mechanics of Laminated Composite Plates and Shells, Theory and Analysis*, CRC Press.
Seide, P. (1958), "Compressive buckling of a long simply supported plate on an elastic foundation", *J. Aerosp. Sci.*, **25**(6), 382-384.
Smith, S.T., Bradford, M.A. and Oehlers, D.J. (1999a), "Elastic buckling of unilaterally constrained rectangular plates in pure shear", *Eng. Struct.*, **21**(5), 443-453.
Smith, S.T., Bradford, M.A. and Oehlers, D.J. (1999b), "Local buckling of side-plated reinforced-concrete beams. I, Theoretical study", *J. Struct. Eng.*, **125**(6), 622-634.
Smith, S.T., Bradford, M.A. and Oehlers, D.J. (1999c), "Local buckling of side-plated reinforced-concrete beams II, Experimental study", *J. Struct. Eng.*, **125**(6), 635-643.
Smith, S.T., Bradford, M.A. and Oehlers, D.J. (1999d), "Numerical convergence of simple and orthogonal polynomials for the unilateral plate buckling problem using the Rayleigh-Ritz method", *Int. J. Numer. Methods Eng.*, **44**(11), 1685-1707.
Timoshenko, S.P. and Gere, J.M. (1936), *Theory of Elastic Stability*, McGraw-Hill, New York, London.
Uy, B. and Bradford, M.A. (1996), "Elastic local buckling of steel plates in composite steel-concrete members", *Eng. Struct.*, **18**(3), 193-200.
Vaseghi, O., Mirdamadi, H.R. and Panahandeh-Shahraki, D. (2013), "Non-linear stability analysis of laminated composite plates on one-sided foundation by hierarchical Rayleigh–Ritz and finite elements", *Int. J. Non-Linear Mech.*, **57**, 65-74.
Weaver, P.M. (2004), "On optimization of long anisotropic flat plates subject to shear buckling loads", *Proceedings of the 45th AIAA/ASME/ASCE/AHS/ACS structures, structural dynamics and materials conference*, Palm Springs, CA, USA, AIAA Paper.
Weaver, P.M. and Nemeth, M.P. (2007), "Bounds on flexural properties and buckling response for symmetrically laminated composite plates", *J. Eng. Mech.*, **133**(11), 1178-1191.
Wright, H. (1993), "Buckling of plates in contact with a rigid medium", *Struct. Eng.*, **71**(12), 209-215.

CC

Appendix A

$$D_{ij} = \frac{1}{3}\sum_{k=1}^{n}(\bar{Q}_{ij})\,(z_k^3 - z_{k-1}^3) \quad i,j = 1,2,6 \tag{A1}$$

$$\bar{Q}_{11} = Q_{11}\,cos^4\,\theta + 2(Q_{12} + 2Q_{66})\,sin^2\,\theta\,cos^2\,\theta + Q_{22}sin^4\,\theta \tag{A2}$$

$$\bar{Q}_{12} = (Q_{11} + Q_{22} - 4Q_{66})\sin^2\theta\cos^2\theta + Q_{12}(\sin^4\theta + \cos^4\theta) \tag{A3}$$

$$\bar{Q}_{16} = (Q_{11} - Q_{22} - 2Q_{66})\sin\theta\cos^3\theta + (Q_{11} - Q_{22} + 2Q_{66})\sin^3\theta\cos\theta \tag{A4}$$

$$\bar{Q}_{26} = (Q_{11} - Q_{22} - 2Q_{66})\sin^3\theta\cos\theta + (Q_{11} - Q_{22} + 2Q_{66})\sin\theta\cos^3\theta \tag{A5}$$

$$\bar{Q}_{22} = Q_{11}\sin^4\theta + 2(Q_{12} + 2Q_{66})\sin^2\theta\cos^2\theta + Q_{22}\cos^4\theta \tag{A6}$$

$$\bar{Q}_{66} = (Q_{11} + Q_{22} - 2Q_{12} - 2Q_{66})\sin^2\theta\cos^2\theta + Q_{66}(\sin^4\theta + \cos^4\theta) \tag{A7}$$

$$Q_{11} = \frac{E_{11}}{1 - \upsilon_{12}\upsilon_{21}} \tag{A8}$$

$$Q_{12} = \frac{\upsilon_{12}E_{22}}{1 - \upsilon_{12}\upsilon_{21}} \tag{A9}$$

$$Q_{22} = \frac{E_{22}}{1 - \upsilon_{12}\upsilon_{21}} \tag{A10}$$

$$Q_{66} = G_{12} \tag{A11}$$

$$\upsilon_{12}E_{22} = \upsilon_{21}E_{11} \tag{A12}$$

where E_{11}, E_{22} and G_{12} are longitudinal modulus, transverse modulus and shear modulus, respectively; ν_{12} and ν_{21} are the corresponding Poisson's ratios; z_k is presented in Fig. 1(b) and θ is the fiber orientation angle.

Appendix B

For the positive shear loading, $\bar{x}_i = x_i - y \cdot c$, where φ is the skewed angle and $c = 1/\tan\varphi$.

Thus, the following equations could be obtained.

$$\begin{aligned}&\left[\alpha^2 + c^2 + \frac{1}{\alpha^2}c^4 - 4\alpha\gamma c - 4\frac{1}{\alpha}\delta c^3\right] f_i'''' \, g \\ &+\left[-4\beta c - 4\frac{1}{\alpha^2}c^3 + 4\alpha\gamma + 12\frac{1}{\alpha}\delta c^2\right] f_i''' \, g' \\ &+\left[2\beta + 6\frac{1}{\alpha^2}c^2 - 12\frac{1}{\alpha}\delta c\right] f_i'' \, g'' \\ &+\left(-4\frac{1}{\alpha^2}c + 4\frac{1}{\alpha}\delta\right) f_i' \, g''' + \frac{1}{\alpha^2} f_i g'''' \\ &+2K\frac{1}{\alpha}\frac{\pi^2}{b^2}(-c f_i'' \, g + f_i' \, g') + k_i f_i g \,/(D_{11}D_{22})^{1/2} = 0\end{aligned} \tag{B1}$$

And then, similar to Eq. (10), Eq. (B1) can be rewritten as

$$\begin{aligned}&B_1\tilde{f}_i''''(\xi_i) - \phi_i{}^2 B_2 \tilde{f}_i''(\xi_i) \\ &+B_3\phi_i{}^4\tilde{f}_i(\xi_i)\left(\frac{1}{\alpha^2} + \tilde{k}_i\right) = 0\end{aligned} \tag{B2}$$

where $B_2 = 24\beta + 72\frac{1}{\alpha^2}c^2 - 144\frac{1}{\alpha}\delta c + 2\frac{1}{\alpha}c\pi^2 K$, $B_3 = 504$, $\tilde{k}_2 = k_r = \frac{b^4 k_2}{504(D_{11}D_{22})^{1/2}}$, for the clamped edges; $B_2 = 2\pi^2\beta + 6\frac{1}{\alpha^2}c^2\pi^2 - 12\frac{1}{\alpha}\delta c\pi^2 + 2\frac{1}{\alpha}c\pi^2 K$, $B_3 = \pi^4$, $\tilde{k}_2 = k_r = \frac{b^4 k_2}{\pi^4(D_{11}D_{22})^{1/2}}$ for the simply supported edges.